Stress corrosion crack depth investigation using the time reversed elastic nonlinearity diagnostic

Brian E. Anderson,[1,a)] Lukasz Pieczonka,[2] Marcel C. Remillieux,[3] Timothy J. Ulrich,[3] and Pierre-Yves Le Bas[3]

[1]*Acoustics Research Group, Department of Physics and Astronomy, Brigham Young University, Provo, UT 84602, USA*

[2]*Department of Robotics and Mechatronics, AGH University of Science and Technology, 30-059 Krakow, Poland*

[3]*Geophysics Group (EES-17), MS D446, Los Alamos National Laboratory, Los Alamos, New Mexico 87545, USA*

bea@byu.edu, lukasz.pieczonka@agh.edu.pl, mcr1@lanl.gov, tju@lanl.gov, pylb@lanl.gov

Abstract: Evidence of the ability to probe depth information of stress corrosion cracking (SCC) are presented using the time reversed elastic nonlinearity diagnostic (TREND). Depth estimation of SCC is important to determine when a stainless steel canister has been breached. TREND is a method to focus elastic energy to a point in space in order to probe that point for damage and its' depth penetration is used here to study depth information about SCC. High frequencies are used to probe near the surface, while low frequencies are used to probe deeper into a stainless steel section of a cylinder.

© 2017 Acoustical Society of America

[DHC]

Date Received: August 2, 2016 **Date Accepted:** December 14, 2016

1. Introduction

Stress corrosion cracking (SCC) can occur in stainless steel, including 304L stainless steel, when the steel is exposed to a corrosive environment, such as humid environments near an ocean which might have airborne chlorides. The most susceptible locations on the steel to cracking are regions under higher levels of stress or locations that have residual stresses as a result of welding or cold rolling to form a cylinder, for example. The United States is currently storing spent nuclear fuel in approximately 2000 storage canisters that include a stainless steel layer.[1] SCC in these steel canisters might allow the release of helium and fission gases.[1] It is estimated that once a crack has been initiated, it can penetrate the steel walls in 16 years.[2] In fact a steel tank in Koeberg, South Africa leaked after 17 years of exposure to the corrosive environment encountered near an ocean with high levels of chlorides in the air.[3] Ultrasonic techniques are currently under development to quantify the penetration depth and orientation of SCC. The purpose of this paper is to show evidence of the ability to image the subsurface orientation and depth of a crack. This work is part of a larger effort dedicated to preventing catastrophic events in nuclear spent fuel storage facilities.

Time reversal (TR) is a method of focusing sound energy at a specific location.[4,5] A forward propagation step of the TR process consists of broadcasting a sinusoidal pulse, S_i, from one or more transducers, one at a time, and recording the chirp responses from the ith transducer, $R_{i,j}$, using a scanning laser Doppler vibrometer (SLDV) that has its light focused at the jth point of a region of interest (ROI) on the surface of a sample. The bandlimited impulse response between the ith transducer and the jth point, $h_{i,j}$, is obtained through a cross correlation of S_i and $R_{i,j}$. A TR of $h_{i,j}(t) \rightarrow h_{i,j}(-t)$ is done and the $h_{i,j}(-t)$ signals are amplified and are broadcast simultaneously from their respective ith transducers, producing a spatially localized focus of energy at the jth point of the ROI. Because the focus is spatially localized, amplitude dependent properties of that local region may be determined. The time reversed elastic nonlinearity diagnostic (TREND) is a nondestructive evaluation (NDE) protocol whereby a TR focus is produced at each point in a ROI.[6] TREND has been used to image surficial impact damage,[7] near surficial diffusion bond imperfections,[8] and recently, surficial cracking in carbon fiber reinforced plastic composite plates using an air coupled TR mirror.[9]

Just as a TR focus has a finite spatial surface expression it also has a finite depth penetration below the surface. Because the focus penetrates below the surface, it

[a)]Author to whom correspondence should be addressed.

 © 2017 Acoustical Society of America

should be possible to image features within that finite amount of depth penetration. Remillieux *et al.* quantified the surficial extent and depth penetration by using a combination of experiments and numerical simulations.[10] They found that the surficial extent of the focusing was half of a Rayleigh wavelength, whereas the depth penetration was one-third of a shear wavelength (both quantities defined in terms of the full width at half maximum of the focusing amplitude). Here we use a low frequency to penetrate deeper below the surface to image the crack profile and a high frequency to more accurately image the surficial expression of a crack. These crack features are imaged by plotting the nonlinear second harmonic amplitude for independent TR foci at each inspection point.

2. Experiment setup

A sample with SCC was provided by the Electric Power Research Institute in Charlotte, North Carolina and a detailed description of its creation was provided by Jackson *et al.*[11] The sample is a section of a cylinder with an outer diameter of 30.5 cm (12 in.) and a wall thickness of 2.54 cm (1 in.). The sample was made of 304L stainless steel with the following nominal properties: a Young's modulus of 200 GPa, a Poisson's ratio of 0.24, and a mass density of 8000 kg/m^3. A boiling magnesium chloride ($MgCl_2$) solution was used to accelerate the cracking process on the inside surface of the cylinder. After SCC was induced in the cylinder, it was machined and prepared into smaller samples, approximately 18 cm $\times$ 7.6 cm in length and width, to allow NDE techniques to be tested on the samples. Figure 1 shows a photograph of the sample.

Eight source transducers (25.4 mm diameter, 6.35 mm thick piezoelectric disks, APC International, Ltd., Mackeyville, PA) were epoxied on the thickness portion of the sample. This defines and fixes our source positions. These locations must remain fixed for the forward and backward TR steps. Temporary adhesives or coupling media (e.g., ultrasonic gel) have also been used by the authors for more rapid scans of a sample. The transducers need not be bonded onto any particular surface of the sample provided the sample's attenuation is low. Thus our transducers could have been bonded onto the inside or outside curved surfaces, though flat transducers bonded onto a curved surface may not conduct vibrations as efficiently (curved transducers could be used). The receiver, a non-contact, scanning laser Doppler vibrometer (PSV 400, OFV 5000 controller, Polytec, Inc., Waldbronn, Germany), was positioned at various points within a ROI identified in Fig. 1 by the red solid line. The TR procedure outlined earlier with a forward broadcast step from a source to a receiver and then a backward broadcast step from the same source to the same receiver constitutes so called reciprocal TR experiments.[5,12] The advantage of this procedure is that the focusing of wave energy occurs at the original, user-selected, receiver location. Since the receiver is a SLDV, the laser can be easily repositioned and a new TR experiment may be performed at the new location. This allows focusing elastic wave energy remotely at several points of interest within the ROI.

A 5 cycle pulse signal is used as the source function, with a 100 kHz center frequency for the lower frequency excitation [see Fig. 2(a)] and a 200 kHz center frequency for the higher frequency excitation. During the forward propagation step, the source signal is successively broadcast from individual source transducers using a 12-bit arbitrary waveform generator with sampling frequency of 10 MHz. The response to a pulse signal is recorded by the laser vibrometer [see Fig. 2(b)] with a sensitivity of 5 mm/s/V and bandwidth of 250 kHz using a 14-bit digitizer also sampling at 10 MHz. The generator and digitizer are synchronized such that the source impulse starts at 1.0 ms in the 3.0 ms window, thus the first portion of the received signal $h_{i,j}(-t)$

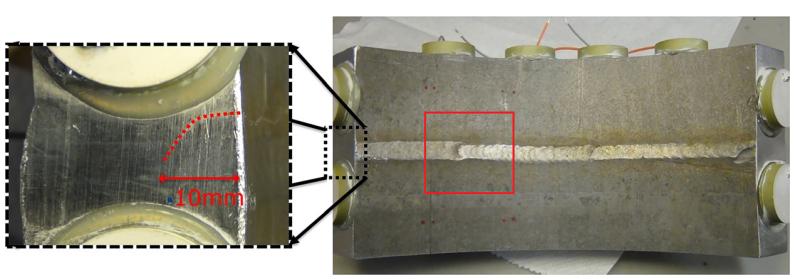

Fig. 1. (Color online) Photograph of the sample under test (on the right). Solid red line colored box indicates the approximate scan area. The dashed line black box (on the left) shows an edge view photograph of the side of the sample with a red dashed line indicating the extent of a barely visible crack.

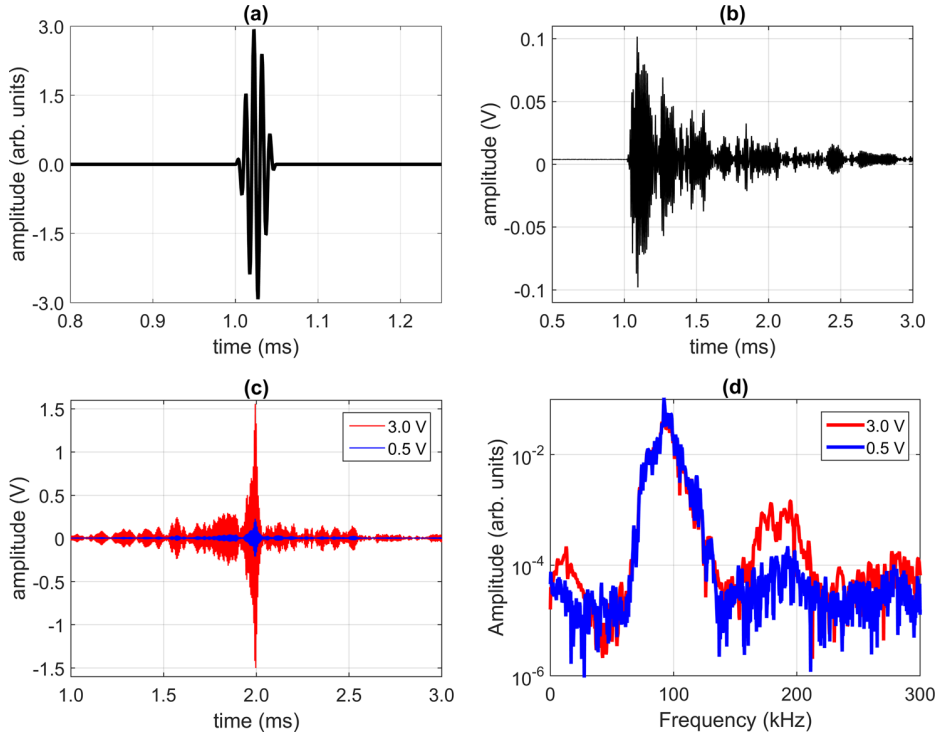

Fig. 2. (Color online) Typical time domain signals of a TR experiment used in this study: (a) 3.0 V, 100 kHz pulse signal broadcast from one source to the laser position; (b) typical received signal by the laser during the forward step; (c) typical TR focal signals obtained by the laser for 0.5 and 3.0 V inputs; (d) typical spectra of the focal signals obtained at a damaged location.

contains no causal signal. This also means that the TR focus ends just prior to 2.0 ms during the rebroadcast [see Fig. 2(c)].

During the backward propagation step, for the jth point, the reversed impulse responses $h_{i,j}(-t)$ are simultaneously broadcast from all eight transducers, which creates a focus of energy at j. Prior to the backward propagation emissions, the $h_{i,j}(-t)$ signals are amplified. Two backward propagation steps are done, one with a lower amplification and one with a higher degree of amplification (see Fig. 2 for example, focal signals). If the focusing to point j is a linear process then these two focal signals should be exactly scalable, aside from background noise. If there is a systematic nonlinearity then perhaps some degree of nonlinearity background will be present at every scan point. Since TR focusing at crack locations was shown to be a nonlinear process, we expect more nonlinearity to be present at a crack location than may be found at other locations that might only have some small amount of system nonlinearity present.

A frequency domain version[9] of the Scaling Subtraction Method (SSM)[13] is conducted to quantify the amount of nonlinearity present between the low and high amplitude focal signals. A Fast Fourier Transform (FFT) is performed on both the low and high amplitude focal signals. The low amplitude spectrum is scaled by the amplification factor difference, s. The SSM calculation sums the FFT magnitudes over certain frequency ranges (between f_1 and f_2) for the low amplitude spectrum, A_f^{low}, and the high amplitude spectrum, A_f^{high}, and performs the following subtraction:

$$\text{SSM} = \sum_{f_1}^{f_2} A_f^{\text{high}} - s \sum_{f_1}^{f_2} A_f^{\text{low}}. \tag{1}$$

For the lower frequency pulse experiment, the fundamental frequency SSM summation spans $f_1 = 70$ kHz and $f_2 = 130$ kHz and for the second harmonic component of the lower frequency pulse experiment the SSM summation spans $f_1 = 170$ kHz and $f_2 = 230$ kHz. For the higher frequency pulse experiment, the fundamental frequency SSM summation spans $f_1 = 150$ kHz and $f_2 = 250$ kHz and for the second harmonic component of the higher frequency pulse experiment the SSM summation spans $f_1 = 350$ kHz and $f_2 = 450$ kHz.

3. Results and discussion

Figure 2(d) displays sample spectra from SSM processing at an intact and a damaged location for the lower frequency pulse excitation only. Note that at the intact location the scaled up low amplitude spectrum essentially matches that of the high amplitude spectrum at both the fundamental frequency and the second harmonic. However at the damaged location, while the fundamental frequency components of both spectra are similar, the high amplitude spectrum clearly contains more second harmonic content than does the scaled up low amplitude spectrum.

Figure 3 displays the spatial mapping of the SSM results for the low and high frequency excitations and for the fundamental and second harmonic frequency summations. The fundamental frequency maps indicate that energy is lost from the fundamental frequency (negative SSM values), which is indicative of nonlinear processes. Neither map of the fundamental frequency component allows accurate visual identification of cracking, aside from relative increases in amplitude reduction in the crack region. However, both of the second harmonic frequency component maps allow identification of a horizontally oriented crack. Note that the second harmonic of the low frequency excitation displays a nonlinear signature that extends from approximately $x = 3$ mm to $x = 16$ mm along the approximate line $y = 24$ mm and another signature that extends from $x = 20$ mm to at least $x = 30$ mm along the approximate line $y = 22$ mm, implying the extent of what may be two cracks. The second harmonic of the high frequency excitation displays a crack feature that extends from approximately $x = 1$ mm to $x = 30$ mm with the range $y = 21$–26 mm. The crack width appears to be smaller for the high frequency excitation. The sample has a very small, though visible, surficial expression of the crack. The crack image in Fig. 3(b) is antisymmetric with respect to the surficial expression of the crack, which also suggests that the crack propagated in the -y direction rather than in the $+y$ direction.

According to Remillieux *et al.*, the penetration depth should be 1/3 of a shear wavelength, or 1.1 cm for 100 kHz and 0.5 cm for 200 kHz in 304 stainless steel (shear wave speed = 3200 m/s).[10] Since the second harmonic frequency content is generated by the crack dynamics of the fundamental frequency vibrations, the penetration depth of the fundamental frequency component should be considered. The image on the left of Fig. 1 suggests that the crack extends perpendicular to the surface for 6 mm before it

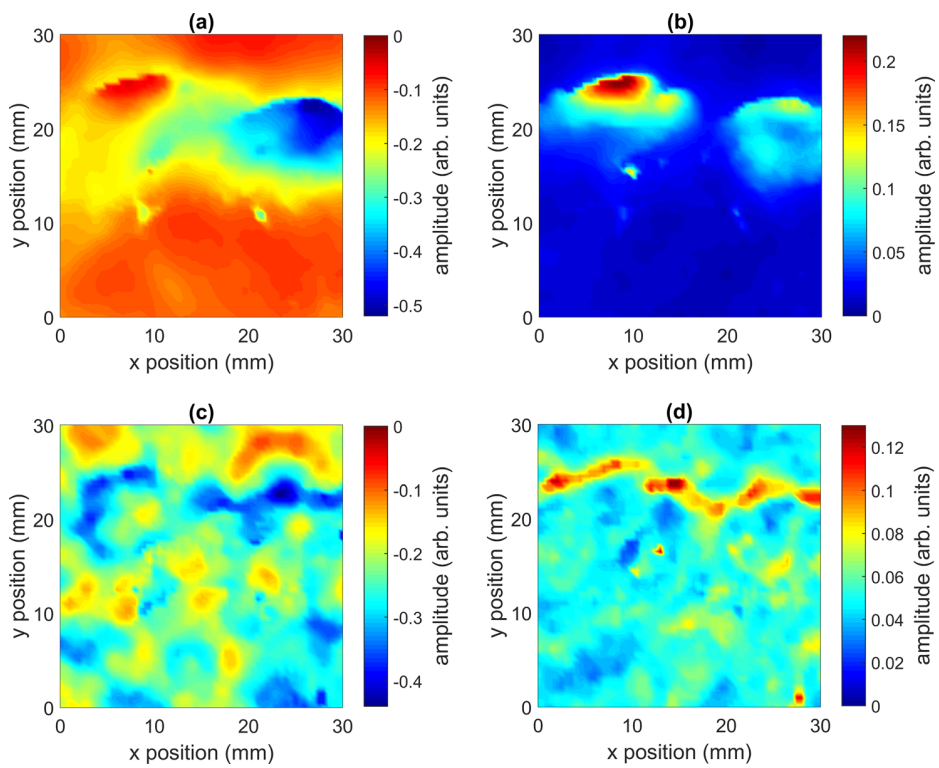

Fig. 3. (Color online) SSM focal maps obtained using the TREND. (a) 100 kHz pulse source excitation, image spans the fundamental band of 70–130 kHz. (b) 100 kHz pulse source excitation, image spans second harmonic band of 170–230 kHz. (c) 200 kHz pulse source excitation, image spans the fundamental band of 150–250 kHz. (d) 200 kHz pulse source excitation, image spans the second harmonic band of 350–450 kHz.

changes directions and extends diagonally for another 8 mm. If we assume that this same crack profile exists at the inspection ROI, since the heat affected zone of the weld should be similar in both cases, then the diagonal extent of the crack should only be able to be imaged with the lower frequency excitation, while the higher frequency excitation can only image the perpendicular orientation portion of the crack.

Thus higher frequencies are able to image near surficial features, while lower frequencies, due to their longer wavelengths, are able to penetrate further below the surface. This has important implications in characterizing the profile of the cracking. The crack orientation can be critical in determining the time before the crack extends through the thickness of the steel wall. In the storage of spent fuel, the concern is not so much to avoid compromising the structural integrity of the canister, but rather to prevent cracking that may allow leaking of gases.

A tradeoff exists in the detection of the presence of the cracking. Lower frequencies not only penetrate deeper below the surface but also have a greater surficial extent. Remillieux *et al.* showed that the surficial extent is approximately 1/2 of a Rayleigh wavelength,[10] or 1.5 cm for 100 kHz and 0.7 cm for 200 kHz (Rayleigh wave speed = 2900 m/s). Lower frequencies might be more ideal for initial inspection of the surface of a sample since the TR focus has a wider surficial extent and therefore does not require the same spatial scanning resolution. The smaller TR focal extent of higher frequencies means that the scan density must increase to avoid missing the detection of a smaller crack feature.

It should be noted that there exist system nonlinearities from the amplifier used, contact nonlinearity between the transducer and the sample, and some amount of nonlinearity from sound propagation through the sample. We assume that these nonlinearities would have essentially equal contributions to second harmonic amplitudes, for example, at any point on a relatively small sample. Essentially these other sources of nonlinearity provide a background noise level for second harmonic imaging. Since TREND maps out the amplitudes as a function of space, any relative increases in nonlinearity at particular locations on the sample are likely due to locally generated distortions, such as the dynamics of crack vibrations, allowing us to image cracks.

4. Conclusions

TREND has been shown to image different features of SCC as a function of depth using different excitation frequencies. The fundamental frequency amplitude decreases at a crack location, shifting energy to harmonic frequencies. High frequencies do not penetrate very far below the surface and are thus able to detect near surficial features of cracking. As the excitation frequency is decreased the TR focus is able to penetrate deeper below the surface and image subsurface changes in the profile of the cracking. Knowledge of the TR focal depth allows quantification of transitions in the crack profile. The exact extent of the crack has not been quantified here and should be studied in future work using destructive tests.

Acknowledgments

This work was funded by the U.S. Department of Energy, Fuel Cycle R&D, Used Fuel Disposition (Storage) Campaign and by the Polish National Science Center under the Grant No. 2015/19/D/ST8/01905. Significant portions of this work were conducted while B.E.A. was employed at Los Alamos National Laboratory.

References and links

[1]E. Gray, "Coast to coast spent fuel dry storage problems and recommendations," in *Division of Spent Fuel Management Regulatory Conference* (Nov. 2015), http://www.nrc.gov/public-involve/conference-symposia/dsfm/2015/dsfm-2015-erica-gray.pdf (Last viewed June 6, 2016).

[2]K. L. Banovac, "Summary of August 5, 2014, public meeting with the nuclear energy institute on chloride induced stress corrosion cracking regulatory issue resolution protocol," U.S. Nuclear Regulatory Commission Public Meeting (August 2014), http://pbadupws.nrc.gov/docs/ML1425/ML14258A081.pdf (Last viewed June 6, 2016).

[3]D. S. Dunn, "Chloride-induced stress corrosion cracking tests and example aging management program," U.S. Nuclear Regulatory Commission Public Meeting (August 2014), http://pbadupws.nrc.gov/docs/ML1425/ML14258A082.pdf (Last viewed June 6, 2016).

[4]M. Fink, "Time reversed acoustics," Phys. Today **50**(3), 34–40 (1997).

[5]B. E. Anderson, M. Griffa, C. Larmat, T. J. Ulrich, and P. A. Johnson, "Time reversal," Acoust. Today **4**, 5–16 (2008).

[6]T. J. Ulrich, P. A. Johnson, and A. Sutin, "Imaging nonlinear scatterers applying the time reversal mirror," J. Acoust. Soc. Am. **119**(3), 1514–1518 (2006).

[7]T. J. Ulrich, P. A. Johnson, and R. A. Guyer, "Interaction dynamics of elastic waves with a complex nonlinear scatterer through the use of a time reversal mirror," Phys. Rev. Lett. **98**, 104301 (2007).

[8]T. J. Ulrich, A. M. Sutin, T. Claytor, P. Papin, P.-Y. Le Bas, and J. A. TenCate, "The time reversed elastic nonlinearity diagnostic applied to evaluation of diffusion bonds," Appl. Phys. Lett. **93**(15), 151914 (2008).

[9]P.-Y. Le Bas, M. C. Remillieux, L. Pieczonka, J. A. Ten Cate, B. E. Anderson, and T. J. Ulrich, "Damage imaging in a laminated composite plate using an air-coupled time reversal mirror," Appl. Phys. Lett. **107**(18), 184102 (2015).

[10]M. C. Remillieux, B. E. Anderson, T. J. Ulrich, P.-Y. Le Bas, and C. Payan, "Depth profile of a time-reversal focus in an elastic solid," Ultrasonics **58**, 60–66 (2015).

[11]B. K. Jackson, D. A. Bosko, M. T. Cronin, J. L. W. Warwick, and J. J. Wall, "Detection of incipient SCC damage in primary loop piping using fiber optic strain gages," in *Proceedings of ASME Pressure Vessels and Piping Conference*, PVP2014-28979 (2014).

[12]B. E. Anderson, M. Griffa, T. J. Ulrich, and P. A. Johnson, "Time reversal reconstruction of finite sized sources in elastic media," J. Acoust. Soc. Am. **130**(4), EL219–EL225 (2011).

[13]M. Scalerandi, A. S. Gliozzi, C. L. E. Bruno, D. Masera, and P. Bocca, "A scaling method to enhance detection of a nonlinear elastic response," Appl. Phys. Lett. **92**(10), 101912 (2008).